



LUND UNIVERSITY
Faculty of Medicine

LU:*research*

Institutional Repository of Lund University

This is an author produced version of a paper published in Tidskriftstitel. This paper has been peer-reviewed but does not include the final publisher proof-corrections or journal pagination.

Citation for the published paper:
Pasupuleti, Mukesh and Walse, Bjorn and Nordahl, Emma and Morgelin, Matthias and Malmsten, Martin and Schmidtchen, Artur.

"Preservation of antimicrobial properties of complement peptide C3a - from invertebrates to humans. "
Journal of Biological Chemistry, 2007, Vol: 282,
Issue: 4, pp. 2520-8.

<http://dx.doi.org/10.1074/jbc.M607848200>

Access to the published version may
require journal subscription.
Published with permission from: American Society for
Biochemistry and Molecular Biology

PRESERVATION OF ANTIMICROBIAL PROPERTIES OF COMPLEMENT PEPTIDE C3a - FROM INVERTEBRATES TO HUMANS

Mukesh Pasupuleti¶, Björn Walse‡, Emma Andersson Nordahl¶, Matthias Mörgelin†, Martin Malmsten§, and Artur Schmidtchen¶||

From the ¶Section of Dermatology and Venereology, †Section of Clinical and Experimental Infectious Medicine, Department of Clinical Sciences, Lund University, Biomedical Center, Tornavägen 10, SE-221 84 Lund, ‡SARomics AB, P. O. Box 724, SE-220 07 Lund, §Department of Pharmacy, Uppsala University, Sweden

Running title: Structural conservation of antimicrobial C3a

|| To whom correspondence should be addressed: Section of Dermatology and Venereology, Department of Clinical Sciences, Lund University, Biomedical Center, Tornavägen 10, SE-22184 Lund, Sweden. Tel: +46462224522; Fax: +4646157756; E-mail: artur.schmidtchen@med.lu.se

The human anaphylatoxin peptide C3a, generated during complement activation, exerts antimicrobial effects. Phylogenetic analysis, sequence analyses and structural modeling studies, paired with antimicrobial assays of peptides from known C3a sequences showed that, in particular in vertebrate C3a, crucial structural determinants governing antimicrobial activity have been conserved during evolution of C3a. Thus, regions of the ancient C3a from *Carcinoscorpius rotundicauda*, as well as corresponding parts of human C3a, exhibited helical structures upon binding to bacterial lipopolysaccharide, permeabilised liposomes, and were antimicrobial against Gram-negative and Gram-positive bacteria. Human C3a and C4a, but not C5a were antimicrobial, in concert with the separate evolutionary development of the chemotactic C5a. Thus, the results demonstrate that, notwithstanding a significant sequence variation, functional and structural constraints imposed on C3a during evolution have preserved critical properties governing antimicrobial activity.

In vertebrates, the complement system is activated by the classical, alternative, and lectin pathways, each converging at the step of C3 with release of multiple proteolytic fragments, including the anaphylatoxin C3a (1). In addition to its multiple proinflammatory functions, involving histamine release from mast cells, smooth muscle contraction, and increased vascular permeability

(1), C3a exerts a direct and potent antimicrobial effect against Gram-negative and Gram-positive bacteria (2). C3 deficiency is connected with increased susceptibility to bacterial infections in humans (3) as well as in animal models (4,5), findings compatible with this direct antibacterial effect of C3a (5). Thus, C3a, in concert with other antimicrobial peptides (AMP) execute pivotal roles in the innate immune system, providing a rapid and non-specific response against potentially invasive pathogenic microorganisms (6). It has been demonstrated that cathelicidins and defensins (for review see (6-8)), representing two important AMP families, display a wide sequence heterogeneity, thus reflecting positive selection and an adaptation of organisms to various bacterial environments (9-11). The complement factor C3 represents an evolutionary old molecule (12), identified in the deuterostome *Ciona intestinalis* (13) as well as in the horseshoe crab, *Carcinoscorpius rotundicauda*, a protostome considered a "living fossil", originating over 500 million years ago (14). These animals, which lack adaptive immunity, mount an effective antimicrobial defense in response to pathogens. In this work, utilizing a combination of phylogenetic studies, structural and sequence alignments paired with biophysical and functional analyses, we show that structural prerequisites governing antimicrobial activity can be traced from the human C3a molecule back to C3a molecules of invertebrates, such as those found in *C. rotundicauda*.

EXPERIMENTAL PROCEDURES

Microorganisms – *Escherichia coli* 37.4, *Enterococcus faecalis* 2374, and *Pseudomonas aeruginosa* 27.1, *Escherichia coli* ATCC 25922, *Bacillus subtilis* ATCC 6633, and *Candida albicans* ATCC 90028 were obtained from the Department of Microbiology, Lund University, Lund.

Peptides and proteins – C3a and C4a were obtained from The Binding Site Inc. (San Diego, CA), while C5a-des Arg was from Calbiochem (San Diego, CA). The peptides GKE31, LGE33, CNY21, CQF20, CVV20 (for sequences see Fig. 2) and tetramethylrhodamine (TAMRA) conjugated CNY21 and CQF20 were synthesized by Innovagen (Lund, Sweden). The purity (>95%) and molecular weight of these peptides was confirmed by mass spectral analysis (MALDI.TOF Voyager). 20mer peptides corresponding to various regions of C3a (Fig. 2 and Table 2, Supporting information) were from Sigma (PEPscreen®, Custom Peptide Libraries, SigmaGenosys, UK).

Phylogenetic analyses – C3a, C4a and C5a amino acid sequences were retrieved from the NCBI site. Each sequence was analyzed with the Psi-Blast (NCBI) (15) for finding the ortholog and paralog sequences. Sequences, which showed structural homology above 70% were selected. These sequences were aligned using clustalW (16), using Blosum 69 protein weight matrix settings (17). Internal adjustments were made, taking the structural alignment into account, utilizing the clustalW interface (<http://bioweb.pasteur.fr/seqanal/interfaces/clustalw.html>). The level of consistency of each position within the alignment was estimated by alignment evaluating software Tcoffee (www.igs.cnrs-mrs.fr/Tcoffee/tcoffee.cgi/index.cgi) (18). C3a, C4a and C5a sequences were used for phylogenetic tree construction by using the neighbour-joining method (19). The generated tree was rooted with human C3a, and the reliability of each branch was assessed using 1000 bootstrap replications. For determination of non-synonymous (amino-acid altering) and synonymous (silent) nucleotide substitutions (dN and dS) (20) we used the codeml PAML available at (<http://abacus.gene.ucl.ac.uk/software/paml.html>). cDNA sequences corresponding to the various C3a peptides of vertebrates were downloaded from the NCBI site (Table 1, Supporting information).

Molecular modeling – A comparative homology model of *C. rotundicauda* C3a was created based on the structure of human C3a (Protein Data Bank code 2A73 (21)). The sequence of human C3a

(residues 651-719 in C3, corresponding to 2-70 in C3a) was aligned against the sequence of *C. rotundicauda* C3a using the alignment in Fig. 2. For clarity, amino acid numbering in the text below is based on the the position in the respective anaphylatoxin peptide, defining the N-terminus after the RKKR processing site. Structural alignment of C3a and C5a structures revealed that the regions corresponding to R8-Y15, L19-M27 and K50-L63 in human C3a (Fig. 2) correspond to structure conserved regions (SCR's). Residues I2 to N67 of *C. rotundicauda* C3a were built using the Prime module (22) from the Schrödinger computational chemistry suite of programs (Schrödinger, L.L.C., Portland, OR, USA). The sequence identity was 26% (similarity 38%) and rotamers from the conserved residues was retained. Terminal tails beyond secondary structure elements were not built. Loops 1 (E11-R13) and 2 (D27-R29) were refined one at a time using default sampling in the loop refinement protocol built into Prime except the long inserted loop 3 (E39-E47), there extended medium sampling was used. Disulfur bridges C17-C49, C18-C56 and C31-C57 were built and minimized prior to refinement. A stepwise refinement protocol involving minimization of (a) side chains from non-SCR regions, (b) both backbone and side chains from non-SCR regions and (c) all side chains were employed. The refined comparative model of *C. rotundicauda* C3a was extended in the C-terminus by residues I68-R75. These residues were added in an α -helical conformation and minimized. Some adjustment of the psi/phi values of L64, L65, K66 and N67 to helical values were necessary prior to minimization. All atoms of residues L64-R75 were minimized of this extended model. Finally all side chains were minimized resulting in the described model. Minimization was performed using the MacroModel module from the Schrödinger computational chemistry suite of programs using a dielectric constant of 1 and the OPLS2005 force field. Comparative homology models of human C4a (residues 1-77) and *Ciona intestinalis* C3a (residues 2-76) were constructed using the same template, refinement protocol and minimization as above and the alignment in Fig. 2. The last seven and five residues, respectively, were added in α -helical conformations and minimized. Sequence identities were 29% (51% similarity) for human C4a and 17% (37% similarity) for *Ciona intestinalis* C3a when compared to human C3a.

Radial-diffusion assay (RDA) – Essentially as described earlier (23), bacteria were grown to mid-log phase in 10 ml of full-strength (3% w/v) trypticase soy broth (TSB) (Becton-Dickinson, Cockeysville, MD). The microorganisms were washed once with 10 mM Tris, pH 7.4. $1-2 \times 10^6$ bacterial colony forming units (CFU) were added to 5 ml of the underlay agarose gel (0.03% TSB, 1% low electro endosmosis type (EEO) agarose (Sigma, St Louis MO) and 0.02% Tween 20 (Sigma)). The underlay was poured into a Ø85 mm petri dish (or Ø 144 mm for the experiment with PEPscreen peptides). After agarose solidification, 4 mm-diameter wells were punched and 6 µl of test peptide was added to each well. Plates were incubated at 37°C for 3 hours to allow diffusion of the peptides. The underlay gel was then covered with 5 ml of molten overlay (6% TSB and 1% Low-EEO agarose in dH₂O). Antimicrobial activity of a peptide is visualized as a zone of clearing around each well after incubating 18-24 hours at 37°C. The activity of the human complement-derived peptides LGE33, CNY21, CQF21, CVV20, and as well as GKE31 of *C. rotundicauda* (at 50 and/or 100 µM) were compared with the activity of the peptide LL-37. In all cases, triplicate samples were used.

Viable-count analysis – *P. aeruginosa* 27.1 or *E. faecalis* 2374 bacteria were grown to mid-logarithmic phase in Todd-Hewitt (TH) medium. Bacteria were washed and diluted in 10 mM Tris, pH 7.4 containing 5 mM glucose. For dose-response experiments *P. aeruginosa* (50 µl; 2×10^6 CFU/ml) were incubated, at 37°C for 2 hours with the peptides GKE31 and LGE33 (*P. aeruginosa*) at concentrations ranging from 0.03 to 60 µM. For analysis of effects of C3a, C4a and C5a-des Arg, (Fig. 6A) *P. aeruginosa* and *E. faecalis* 2374 were used and the peptide concentration was 3 µM. To quantify the bactericidal activity, serial dilutions of the incubation mixture were plated on TH agar, followed by incubation at 37°C overnight and the number of cfu was determined.

Electron microscopy – *P. aeruginosa* 27.1 ($1-2 \times 10^6$ /sample) were incubated for 2 hours at 37°C with the peptides GKE31 or LGE33 at ~90% of their required bactericidal concentration (6 µM), as judged by dose-response experiments using viable count assays (not shown). LL-37 (6 µM) was included as a control. Samples of *P. aeruginosa* bacteria suspensions were adsorbed onto carbon-coated copper grids for 2 min, washed briefly on two drops of water, and negatively stained on two drops of 0.75 % uranyl formate. The grids were

rendered hydrophilic by glow discharge at low pressure in air. Specimens were observed in a Jeol JEM 1230 electron microscope operated at 60 kV accelerating voltage. Images were recorded with a Gatan Multiscan 791 CCD camera.

CD-spectroscopy – The CD spectra of the peptides in solution were measured on a Jasco J-810 Spectropolarimeter (Jasco, U.K.). The measurements were performed at 37°C in a 10 mm quartz cuvet under stirring and the effect on peptide secondary structure was monitored in the range 200-250 nm. The background value (detected at 250 nm, where no peptide signal is present) was subtracted and signals from the bulk solution were corrected for. The peptide secondary structure was monitored at a peptide concentration of 10 µM, both in Tris buffer and in the presence of *E. coli* lipopolysaccharide (0.02 wt%) (*Escherichia coli* 0111:B4, highly purified, less than 1% protein/RNA, Sigma, UK)

Liposome preparation and leakage assay – Dry lipid films were prepared by dissolving either dioleoylphosphatidylcholine (Avanti Polar Lipids, Alabaster, AL) (60 mol%) and cholesterol (Sigma, St Louis, MO) (40 mol%), or dioleoylphosphatidylcholine (30 mol%), dioleoylphosphatidic acid (Avanti Polar Lipids, Alabaster, AL) (30 mol%) and cholesterol (40 mol%) in chloroform, and then removing the solvent by evaporation under vacuum overnight. Subsequently, buffer (10 mM Tris, pH 7.4) was added together with 0.1 M carboxyfluorescein (CF) (Sigma, St Louis, MO). After hydration, the lipid mixture was subjected to eight freeze-thaw cycles consisting of freezing in liquid nitrogen and heating to 60°C. Unilamellar liposomes, of about Ø100 nm were generated by multiple extrusions through polycarbonate filters (pore size 100 nm) mounted in a LipoFast miniextruder (Avestin, Ottawa, Canada) at 22°C. Untrapped carboxyfluorescein was then removed by two gel filtrations (Sephadex G-50) at 22°C, with the Tris buffer as eluent. The CF release was determined by monitoring the emitted fluorescence at 520 nm from a liposome dispersion (10mM lipid in 10 mM Tris pH 7.4). An absolute leakage scale is obtained by disrupting the liposomes at the end of the experiment through addition of 0.8 mM Triton X100 (Sigma, St Louis, MO), thereby causing 100% release and dequenching of CF. A SPEX-fluorolog 1650 0.22-m double spectrometer (SPEX Industries, Edison, NJ) was used for the liposome leakage assay.

Fluorescence microscopy – P. aeruginosa 27.1 bacteria were grown to mid-logarithmic phase in TH medium. The bacteria were washed twice in 10 mM Tris, pH 7.4. The pellet was dissolved to yield a suspension of 5×10^6 cfu/ml in the same buffer. Two hundred microliter of the bacterial suspension was incubated with either 1 μ l TAMRA-CNY21 or TAMRA-CQF21 (2 mg/ml) on ice for 5 min and washed twice in 10 mM Tris, pH 7.4. The bacteria were then fixed by incubation on ice for 15 min and in room temperature for 45 min in 4% paraformaldehyde. The suspension was applied onto Poly-L-lysine coated cover glass and bacteria were let to attach for 30 min. The liquid was poured away and the cover glass was mounted on a slide by Dako mounting media, Dako (Carpinteria, CA). This was performed using a Nikon Eclipse TE300 inverted fluorescence microscope equipped with a Hamamatsu C4742-95 cooled CCD camera, a Plan Achromat 60X objective, and a high N.A. oil-condenser.

Supplementary data – Supplementary data is available at *JBC* Online.

RESULTS

Sequence analyses of anaphylatoxin homologues – Phylogenetic analysis of representative C3a peptides from invertebrates as well as vertebrates (Fig. 1) yielded valuable information. Consistent with a common ancestor, the C3a molecules all colocalized to a single group, suggesting that C3a has evolved via multiple changes in the protogene, a finding consistent with previous analyses of the evolution of the complement system (14,24). On the other hand, C4a and C5a formed separate clades, C5a being most distant from the C3a. This pattern suggests that C5a and C4a likely evolved from C3a and that C5a is the paralog to C4a and C3a (14). Comparisons of synonymous and nonsynonymous substitution rates are useful for studying the mechanisms of gene evolution. Analysis of evolutionary distant sequences, however, is not useful due to saturation of amino acid changes. Nevertheless, in order to get useful information on possible positive selection of C3a, relevant and homologous vertebrate sequences were compared. The dS values (indicating synonymous nucleotide substitutions) ranged 0.7-1.0, except for *Macropus eugenii*, which showed a higher substitution rate around 2.7, whereas the dN (indicating nonsynonymous substitutions) ranged 0.1-0.2 (Table 1, Supplementary data). Thus, albeit the existence of an extensive variability of certain

amino acids in C3a (Fig. 2), the results from the analysis of vertebrate sequences indicate that the selection pressure imposed on the C3a molecules, results in a high degree of conservation.

Given this phylogenetic relation, it was of interest to examine this molecular family closer, both from a structural as well as functional perspective. Several common structural features exist for the corresponding C3a, C4a, and C5a sequences of various organisms, crucial for the integrity and stability of the molecules (Fig. 2). A most notable feature is the existence of six disulfide-bonded cysteines, which are conserved not only in C3a, but also in C4a and C5a. The three disulfide bonds stabilize the conformation of the internal "core" portion of the molecules, represented by residues 22-57 in the human C3a sequence. The C3a of *Ciona intestinalis* lacks one disulfide pair (Fig. 2) and will be discussed separately below. Focusing on C3a, it is evident that apart from cysteines, the four glycines (positions 13, 26, 46, 74), phenylalanine (53), as well as lysines and arginines (21, 64, 77) constitute additional conserved features, suggesting their importance for the structural stability as well as function of C3a.

Structural modeling of anaphylatoxin peptides – Computational modeling, utilizing available structural data on human C3a (21,25) as well as C5a peptides (26,27), was employed to provide further structural information. Considering the recent identification of C3, and a putative anaphylactic peptide in the arthropod *C. rotundicauda* (14), we decided to compare these two molecules. As demonstrated in Fig. 3A, the similarity at the 3-D level between human C3a and the predicted *C. rotundicauda* C3a peptide is apparent, albeit an extensive overall sequence discrepancy (26% sequence identity and 38% similarity). Both peptides share a striking similarity in the four helical regions and in the two first loops located before the cysteines at positions 22 and 36 and positions 17 and 31 in the human and *C. rotundicauda* peptides, respectively. The *C. rotundicauda* C3a has a five amino acid long insert in the third loop region between the cysteines at positions 31 and 49, a feature only shared with C3a from *C. intestinalis*. Analogously to human C3a, the *C. rotundicauda* peptide contains a prominent cationic and amphipathic helical C-terminus, predicted to extend a few residues further than in human C3a. In human C3a, the C-terminal part of this region, being flexible in solution, strongly conforms to an α -helical conformation in anisotropic

environments (1). Helical wheel diagrams (Edmundson projection) illustrate the amphipathic nature of the C-terminal helices (given a helical conformation) (Fig. 3B), as defined by the peptides GKE31 and LGE33 which encompass this region of *C. rotundicauda* and human C3a, respectively (see Fig. 2 for sequence). The amphipathic organisation of these helices is also seen in the 3-D models of *C. rotundicauda* and human C3a (Fig. 3A).

Antimicrobial activities of C3a peptides – In order to explore the structure-function relationships of C3a epitopes, overlapping peptide sequences comprising 20mers (Fig. 2 and Table 2, Supplementary data) were synthesized and screened for antimicrobial activities against *P. aeruginosa*, a ubiquitous pathogen found among both vertebrates as well as invertebrates. The experiments showed that particularly peptides derived from the C-terminal regions of *C. rotundicauda*, *Ciona*, and *Branchiostoma*, as well as from the vertebrates *Homo*, *Sus*, *Mus*, *Rattus*, and *Guinea*, were antimicrobial (Fig. 4), whereas peptides originating from *Cobra*, *Paralichthys*, *Onchorhynchus*, *Eptatretus*, *Xenopus*, and *Gallus* did not show any activity against bacteria (Fig. 4). Properties common for most AMPs include minimum levels of cationicity, amphipathicity, and hydrophobicity (6). Therefore, it was interesting to note that C-terminal regions of the two former groups comprised cationic peptides, whereas the latter group comprised negatively charged peptides (illustrated by colors in Fig. 4). These results corresponded well with the phylogenetic analysis, which showed that these animals belong to different subclades and with single nodes of divergence (Fig. 1). The global analysis of biophysical parameters showed that in general, peptides displaying antimicrobial activity had a net charge of +2-+4 and ~20-40% hydrophobic amino acids. The degree of amphipathicity, as judged by the relative hydrophobic moment (μHrel) ranged ~0.2-0.4, values comparable with those observed in many helical AMPs (28). Although intuitively apparent (Fig. 4), the results confirmed that net charge correlates to antimicrobial activity (Fig. 1, Supplementary data). Considering these findings, it is notable that disproportionate alteration of charge appear to characterize the evolution of β -defensins (9,29). Analogous relationships were recently reported to apply to the evolution of primate cathelicidin, showing positive selection affecting charge while keeping hydrophobicity and amphipathicity fairly constant (11).

Structural and functional congruence of C-termini of C3a – In humans, peptides derived from

the well-defined C-terminal region of C3a exert antimicrobial effects. Furthermore, human neutrophilic enzymes release similar C3a-derived peptides exerting antimicrobial effects, proving the physiological importance of this helical and antimicrobial region of C3a (2). Considering this, the following experimental analyses focused on the C-terminal region of human C3a as well as the related peptide "ancestor" from *C. rotundicauda* (see Fig. 2 and Fig. 3B). Indeed, the experiments showed that the *C. rotundicauda* peptide GKE31, spanning the whole C-terminal part of *C. rotundicauda* C3a, exerted similar antibacterial effects as the human homolog LGE33 against both the Gram-negative *P. aeruginosa* and *E. coli* and the Gram-positive *Bacillus subtilis* (Fig. 5A). The "classical" human cathelicidin LL-37 yielded similar effects as the two C3a-derived peptides. The *C. rotundicauda* peptide was not active against *Candida albicans*. To examine whether the GKE31 and LGE33 peptides interact with and permeabilize bacterial plasma membranes, *P. aeruginosa* was incubated with each of the two peptides at concentrations yielding ~90 % bacterial killing (6 μM), and analyzed by electron microscopy (Fig. 5B). Clear differences in the morphology of peptide-treated bacteria in comparison with the control were demonstrated by this approach. The peptides caused local perturbations and breaks along *P. aeruginosa* plasma membranes, and occasionally, intracellular material was found extracellularly. These findings were similar to those seen after treatment with the antimicrobial human cathelicidin LL-37 (Fig. 5B). Furthermore, circular dichroism (CD) spectroscopy was used to study the structure and the organization of the GKE31 and LGE33 peptides in solution and upon interaction with *E. coli* LPS (Fig. 5C). Neither GKE31 nor LGE33 adopted an ordered conformation in aqueous solution, however the CD spectra revealed that a significant and almost identical structural change, largely indicating an induction of helicity, taking place in the presence of *E. coli* LPS (Fig. 5C). The remarkably similar profile of both peptides indicates that despite a marked difference in primary sequence, the peptides structure in a similar way in presence of negatively charged LPS-rich bacterial membranes. Both the peptides also induced leaking of liposomes, thus establishing their membrane breaking activities (Fig 5D). Kinetic analysis showed that ~80% of the maximum fluorescence was reached within ~200 seconds for both peptides (at 1 μM) (Fig. 5E). The results

therefore indicate that the GKE31 and LGE33 peptides indeed function like most helical AMPs such as LL-37 (6,28), by interactions with LPS and most likely, peptidoglycan at bacterial surfaces, leading to induction of an α -helical conformation, which in turn facilitates membrane interactions, membrane destabilization and finally, bacterial killing. The fact that the two C3a-derived peptides are separated by as much as over a half billion years of evolutionary distance elegantly demonstrate the remarkable structural and functional conservation of this C-terminal peptide region.

Comparison of C3a molecules of C. rotundicauda and C. intestinalis – The C3a molecule of *Ciona* is functionally active; it exerts chemotactic effects (13), and as shown here, has a C-terminal antibacterial part (Fig. 4). However, in contrast to the other C3a molecules, C3a of *Ciona* lacks one disulfide bridge (Fig. 2). Despite this, and a sequence identity of only 17% (37% similarity) with human C3a, molecular modeling and conformational analysis show that *Ciona* C3a adopts a predicted conformation similar to other C3a molecules (Fig. 6A). Interestingly, the first missing cysteine in *Ciona* C3a is replaced by a glycine residue (Gly 18), whereas the second cysteine is replaced by a glutamate residue (Glu 57). Hypothetically, these changes could enable the second helix to approach to and interact with the C-terminal helix, by formation of a salt bridge between Glu 57 and Lys 22, thus compensating for the loss of a disulfide bond. These interactions, together with main structural constraints imposed by the remaining two disulfide pairs preserve the overall topology of *Ciona* C3a (Fig. 6B). Furthermore, it is notable that residues forming the inner "core" through out the anaphylatoxin family (Gly 21, Ile/Val 39, and Phe 54) are all conserved in *Ciona* C3a (Fig. 2). Taken together, these structural considerations, combined with the functional data, further underscore the conservation of C3a.

Structure and activities of C4a and C5a – The phylogenetic analysis indicated that C5a evolved separately from the family of C3a as well as C4a molecules (Fig. 1). To address whether this also reflected a functional difference, we compared the antibacterial activities of human C3a, with C4a, and C5a (the latter only available in des-Arg form) and their corresponding peptides from the C-terminus. C3a and C4a both exerted antibacterial effects, whereas the C5a-peptide was inactive (Fig. 7A). Corroborating results were obtained with the corresponding C-terminal peptides (Fig. 7B, for sequences see Fig. 2). Whereas the C3a and C4a-derived peptides (CNY21 and CQF21, respectively)

killed the Gram-negative *P. aeruginosa* and *E. coli*, the Gram-positive *B. subtilis*, as well as the fungus *C. albicans*, the C5a-peptide (CVV20) was inactive against these microbes. The fact that the C5a-derived peptide CVV20 contained a terminal arginine, and that there is no difference in antimicrobial activity between C3a and C3a des-Arg, as well as the corresponding C3a-derived peptides CNY21 and CNY20 (2), demonstrated that the terminal arginine is dispensable for antimicrobial activity of these peptides. Finally, the interaction between the antimicrobial peptides CNY21 (C3a) and CQF21 (C4a) and bacterial plasma membranes was examined by fluorescence microscopy. The peptides were labeled with the fluorescence dye TAMRA and incubated with *P. aeruginosa*. As demonstrated, the peptides bound to the bacterial surface, and the binding was completely blocked by negatively charged glycosaminoglycan heparin (Fig. 7C). As seen in the 3-D models, the last ten residues in C5a form a short α -helix that is bent backwards through a short loop positioning the carboxy terminal arginine (Arg 74) in close proximity to arginine 62 (Fig. 3A), a feature that is believed to be important for receptor binding (27). Thus, C5a display a significantly different structure when compared with both C4a and C3a, lacking the typical C-terminal and antimicrobial protruding peptide (Fig. 3A), thus compatible with the experimental results presented herein. This observation, paired with the separate evolutionary development of C5a, indicate that this molecule has evolved separately in higher organisms into a purely chemotactic and highly spasmogenic molecule.

DISCUSSION

In conclusion, the combination of phylogenetic, structural, biophysical and biological analyses, point at a preservation of structures crucial for antimicrobial activity of C3a in invertebrates as well as vertebrate lineages. Although speculative, the difference noted in C3a of jawless fishes, likely abolishing C3a's antimicrobial activity, may not only reflect the multifunctional role of C3a, but could also indicate a gain of other functions during the separation from invertebrates in the ordovician period (500 million years ago). The observation that anaphylatoxins have unforeseen biological effects in fish, is compatible with this hypothesis (30). As mentioned previously, significant changes in cationicity are observed in defensins

as well as cathelicidins even in closely related species (such as primates) (11,31). Furthermore, indicative of a strong nonneutral evolution, gene duplications and subsequent variations has lead to further generation of different AMPs (29). For example, the C-terminal domains of cathelicidins may range from a dozen to over eighty residues forming cysteine-bridged hairpins (bovine bactenecin), tryptophan-rich (bovine indolicidin), proline-rich (porcine PR-39), or α -helical molecules (human LL-37) (8). In this context it is interesting to note that a unifying structural motif (γ -core) was recently revealed in many diverse AMPs, such as protegrins, defensins and chemokines, thus indicating the existence of previously unprecedented higher level structural

motifs which govern antimicrobial functions (6). Being multifunctional, also acting as immune modulators, the generation of many structurally diverse AMPs likely reflects an evolutionary adaptation to the microbial environment, as well as introduction of novel biological functions, in a given organism. Contrasting to this, C3a has maintained strikingly similar features governing antimicrobial activity, in spite of a significant primary sequence variation. Thus, in addition to Nature's "innovative" generation of AMPs, our findings on C3a illustrate an alternative concept where molecules are subjected to strong and precise selection forces aiming at maintaining a robust and structurally intact innate defense system.

REFERENCES

1. Hugli, T. E. (1990) *Curr Top Microbiol Immunol* **153**, 181-208
2. Nordahl, E. A., Rydengård, V., Nyberg, P., Nitsche, D. P., Mörgelin, M., Malmsten, M., Björck, L., and Schmidtchen, A. (2004) *Proc Natl Acad Sci U S A* **101**, 16879-16884
3. Alper, C. A. (1998) *Exp Clin Immunogenet* **15**, 203-212
4. Wessels, M. R., Butko, P., Ma, M., Warren, H. B., Lage, A. L., and Carroll, M. C. (1995) *Proc Natl Acad Sci U S A* **92**, 11490-11494
5. Kerr, A. R., Paterson, G. K., Riboldi-Tunnicliffe, A., and Mitchell, T. J. (2005) *Infect Immun* **73**, 4245-4252
6. Yount, N. Y., Bayer, A. S., Xiong, Y. Q., and Yeaman, M. R. (2006) *Biopolymers* **84**, 435-458
7. Zasloff, M. (2002) *Nature* **415**, 389-395.
8. Lehrer, R. I., and Ganz, T. (2002) *Curr Opin Hematol* **9**, 18-22
9. Maxwell, A. I., Morrison, G. M., and Dorin, J. R. (2003) *Mol Immunol* **40**, 413-421
10. Tomasinsig, L., and Zanetti, M. (2005) *Curr Protein Pept Sci* **6**, 23-34
11. Zelezetsky, I., Pontillo, A., Puzzi, L., Antcheva, N., Segat, L., Pacor, S., Crovella, S., and Tossi, A. (2006) *J Biol Chem* **281**, 19861-19871
12. Zarkadis, I. K., Mastellos, D., and Lambris, J. D. (2001) *Dev Comp Immunol* **25**, 745-762
13. Pinto, M. R., Chinnici, C. M., Kimura, Y., Melillo, D., Marino, R., Spruce, L. A., De Santis, R., Parrinello, N., and Lambris, J. D. (2003) *J Immunol* **171**, 5521-5528
14. Zhu, Y., Thangamani, S., Ho, B., and Ding, J. L. (2005) *Embo J* **24**, 382-394
15. Altschul, S. F., Madden, T. L., Schaffer, A. A., Zhang, J., Zhang, Z., Miller, W., and Lipman, D. J. (1997) *Nucleic Acids Res* **25**, 3389-3402
16. Thompson, J. D., Higgins, D. G., and Gibson, T. J. (1994) *Nucleic Acids Res* **22**, 4673-4680
17. Henikoff, S., and Henikoff, J. G. (1992) *Proc Natl Acad Sci U S A* **89**, 10915-10919
18. Poirot, O., Suhre, K., Abergel, C., O'Toole, E., and Notredame, C. (2004) *Nucleic Acids Res* **32**, W37-40
19. Saitou, N., and Nei, M. (1987) *Mol Biol Evol* **4**, 406-425
20. Tennessen, J. A. (2005) *J Mol Evol* **61**, 445-455
21. Janssen, B. J., Huizinga, E. G., Raaijmakers, H. C., Roos, A., Daha, M. R., Nilsson-Ekdahl, K., Nilsson, B., and Gros, P. (2005) *Nature* **437**, 505-511
22. Jacobson, M. P., Pincus, D. L., Rapp, C. S., Day, T. J., Honig, B., Shaw, D. E., and Friesner, R. A. (2004) *Proteins* **55**, 351-367

23. Lehrer, R. I., Rosenman, M., Harwig, S. S., Jackson, R., and Eisenhauer, P. (1991) *J Immunol Methods* **137**, 167-173
24. Nonaka, M., and Yoshizaki, F. (2004) *Mol Immunol* **40**, 897-902
25. Huber, R., Scholze, H., Paques, E. P., and Deisenhofer, J. (1980) *Hoppe Seylers Z Physiol Chem* **361**, 1389-1399
26. Williamson, M. P., and Madison, V. S. (1990) *Biochemistry* **29**, 2895-2905
27. Zhang, X., Boyar, W., Toth, M. J., Wennogle, L., and Gonnella, N. C. (1997) *Proteins* **28**, 261-267
28. Zelezetsky, I., and Tossi, A. (2006) *Biochim Biophys Acta* **1758**, 1436-1449
29. Tennessen, J. A. (2005) *J Evol Biol* **18**, 1387-1394
30. Sunyer, J. O., Boshra, H., and Li, J. (2005) *Vet Immunol Immunopathol* **108**, 77-89
31. Semple, C. A., Rolfe, M., and Dorin, J. R. (2003) *Genome Biol* **4**, R31

FOOTNOTES

*This work was supported by grants from the Swedish Research Council (projects 13471 and 621-2003-4022), the Royal Physiographic Society in Lund, the Welander-Finsen, Söderberg, Schyberg, Groschinsky, Crafoord, Åhlen, Alfred Österlund, Lundgrens, Lions and Kock Foundations, and The Swedish Government Funds for Clinical Research (ALF).

The abbreviations used are: AMP, antimicrobial peptide; C3, complement factor 3; CFU, colony forming units; CF, carboxyfluorescein; RDA, radial diffusion assays; TSB, trypticase soy broth; TH, Todd-Hewitt.

Acknowledgment: We wish to thank Ms. Lotta Wahlberg for expert technical assistance.

FIGURE LEGENDS

Fig. 1. Evolution of anaphylatoxins. Phylogenetic tree presenting C3a, C4a, C5a sequences using the neighbour joining method. Numbers on the branches indicate the reliability of each branch using 1000 bootstrap replications.

Fig. 2. Alignment of C3a, C4a, and C5a sequences showing identical and similar amino acid substitutions. The shading represents the degree of conservation at each position in the alignment, taking into account similar physicochemical properties of the residues. The peptide sequences corresponding to regions 1-6 in the human C3a sequence are indicated. Note that this only applies to the C3a sequences (The full information on these peptides is given in Table 2, Supporting information). The amino termini of peptides LGE33 (C3a *Homo*), CNY21 (C3a *Homo*), CQF21 (C4a *Homo*), CVV20 (C5a *Homo*) and GKE31 (C3a, *C. rotundicauda*) are indicated by an asterisk in the alignments. All peptides terminate at the final arginine residue. Disulfide bonds are indicated (bottom).

Fig. 3. Molecular models of human C3a, C4a, and C5a and *C. rotundicauda* C3a and illustration of amphipathicity of C-terminal peptides of C3a. (A) Molecular models. Human C3a is represented by the corresponding part in the crystal structure of human C3 (PDB code 2A73; (21)). The last seven residues were missing in this structure due to inherent flexibility and were added in an α -helical conformation for comparable purposes. Human C4a and *C. rotundicauda* C3a are represented by homology models based on the crystal structure of human C3a. Human C5a is represented by the NMR structure described in Zhang et al., 1997 (PDB code 1KJS)(27). From top to bottom; Ribbon, front and back surface representations, respectively of *C. rotundicauda* C3a, human C3a, C4a, and C5a. Color coding as follows: blue - positively charged residues (H, K and R); red - negatively charged residues (D and E); cyan - polar residues (C_{SH}, S, N, Q, T, Y, W); green - hydrophobic residues (A, C_{SS}, F, G, I, L, M, P, V). (B) Helical wheel representation of the C3a-derived C-terminal peptides GKE31 (from *C. rotundicauda*) and LGE33 (*Homo*). The amino acids are indicated.

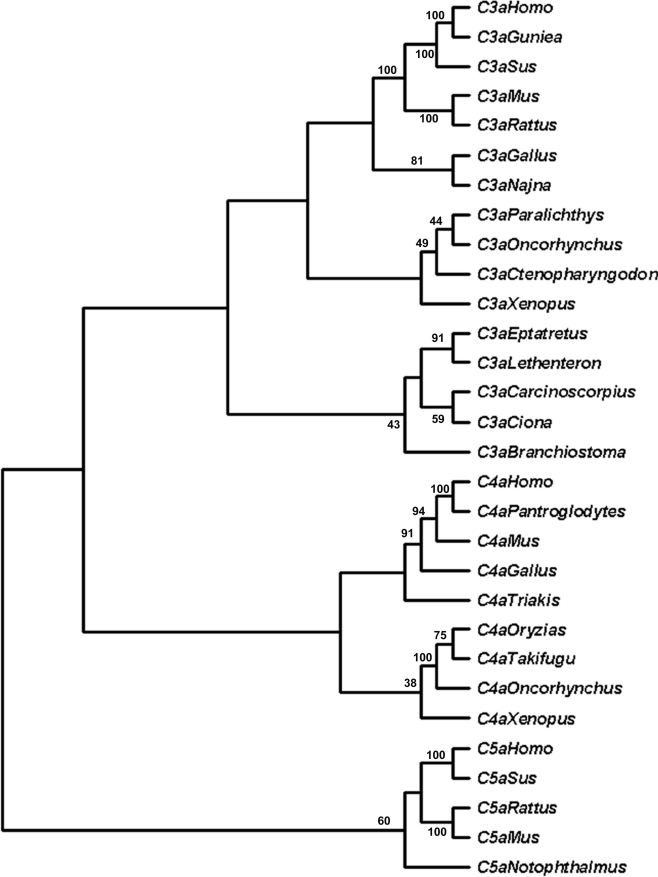
Fig. 4. Antibacterial activities of C3a peptides. Overlapping peptides (regions 1-6, see Fig 2 and also Table 2, Supplemental data) of C3a were analysed for antimicrobial activities against *P. aeruginosa*. The regions, inhibitory zones, the respective organism, as well as net charge of respective peptides are indicated in the 3-D graph. For determination of antibacterial activities, *P. aeruginosa* isolate (4×10^6 cfu) was inoculated in 0.1% TSB agarose gel. Each 4 mm-diameter well was loaded with 6 μ l of peptide (at 200 μ M). The zones of clearance correspond to the inhibitory effect of each peptide after incubation at 37 °C for 18-24 h (mean values are presented, n=3).

Fig. 5. Activities of C3a-derived human and *C. rotundicauda* peptides. (A) Antibacterial effects. Peptides were tested in radial diffusion assay in low-salt conditions. *P. aeruginosa*, *E. coli*, *B. subtilis*, and *C. albicans* (4×10^6 cfu) were inoculated in 0.1% TSB agarose gel. Each 4 mm-diameter well was loaded with 6 μ l of the peptides GKE31 and LGE33 as well as LL-37 peptide at 100 μ M. The zones of clearance (y-axis) correspond to the inhibitory effect of each peptide after incubation at 37 °C for 18-24 h. Mean values and SD are presented (n=3). The inset illustrates the antibacterial effects of the peptides against *P. aeruginosa*. (B) The C3a-derived peptides GKE31 and LGE33 generate breaks in bacterial plasma membranes. *P. aeruginosa* was incubated with GKE31 and LGE33 peptides (at 6.0 μ M) and analyzed with electron microscopy. The peptides are indicated in the figure. The scale bar corresponds to 0.5 μ m. Control; buffer control. (C) CD spectrum of GKE31 and LGE33 in Tris buffer and in presence of LPS. For control, CD spectra for buffer and LPS alone are presented. (D) Effects of GKE33 and LGE31 on liposome leakage. The membrane permeabilizing effect was recorded by measuring fluorescence release of carboxyfluorescein from liposomes. Values represents mean of triplicates samples. (E) Kinetic analysis of liposome permeabilisation using 1 μ M of GKE31 and LGE33 peptides, respectively.

Fig. 6. Molecular model of *Ciona intestinalis* C3a and comparison with *Carcinoscorpius rotundicauda* C3a.

(A) Composite model incorporating *Ciona* C3a (grey) and *C. rotundicauda* C3a (magenta). The location of the missing disulfide bond in *Ciona* C3a is indicated by an arrow. (B) Front and back surface representations of *Ciona* C3a. Color coding as in Fig. 3. Note the amphipathic character of the C-terminal helix.

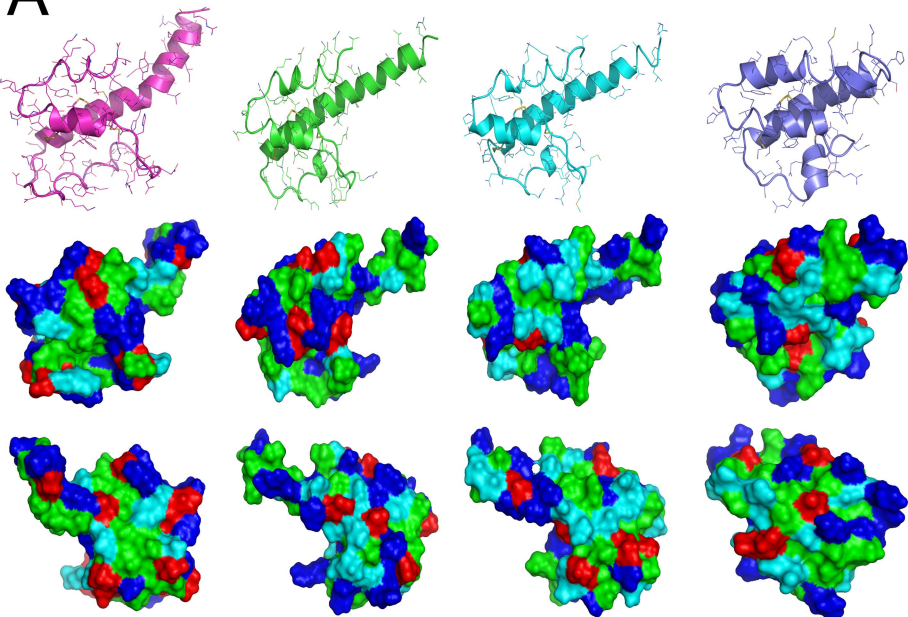
Fig. 7. Activities of human C3a, C4a, and C5a, and related C-terminal peptides. (A) Activities of C3a, C4a, and C5a (as desArg) on *P. aeruginosa* 27.1 and *E. faecalis* 2374. In viable count assays C3 and C4a, but not C5a, displayed antibacterial activities against both bacterial isolates. 2×10^6 cfu/ml of bacteria were incubated in 50 μ l with peptides at a concentration of 3 μ M. (B) Antibacterial activities of synthetic peptides derived from the carboxy-terminal regions of C3a, C4a, and C5a. *P. aeruginosa*, *E. coli*, *Bacillus subtilis* and *Candida albicans* (4×10^6 cfu) were inoculated in 0.1% TSB agarose gel. Each 4 mm-diameter well was loaded with 6 μ l of the peptides CNY21, CQF21, or CVV20 (100 μ M), derived from the carboxyterminus of C3a, C4a, and C5a, respectively. The zones of clearance correspond to the inhibitory effect of each peptide after incubation at 37 °C for 18-24 h. Antibacterial activity is indicated (y-axis). Mean values and SD are presented (n=3). For comparison, LL-37 was used. The inset illustrates the antibacterial effects of the peptides against *P. aeruginosa*. (C) Binding of TAMRA-labeled peptides to *P. aeruginosa* 27.1 and inhibition of binding by excess of heparin. The lower panels shows red fluorescence of bacteria (1×10^7 ml⁻¹) stained with the indicated TAMRA-conjugated peptides (10μ g ml⁻¹) in absence or presence of heparin. All images were recorded using identical instrument settings. The corresponding Nomarski images are shown in the upper panel. Scale bar represents 10 μ m.



650 670 690 710 726

-SVQTEKRMDKVGKYP-KELR-KCEDGMREN* -RRFSORRRTFISL* -GEAKKQVELDCCNYITELRRQHRARASH-LGLAR 726
 -SVQTEKRMDKAGKYKSKELR-KCEDGMREN* -MQFSORRRTYVSL* -GEAVKAFLDCCTYMAQLRQHRREQN-LGLAR
 -SVQTEKRMDKLGQYS-KELR-KCEHGMRNP -MKFSORRRAOFIHQ -GNAVKAFLNCCFYIAKLRQHSRKNP-LGLAR
 -SVQTEKRMDKAGQYTDKGLR-KCEDGMRDIP -MRYSCORRRLITQ -GENSIKAFIDCCNHITKLRQHRRDHV-LGLAR
 -SVQTEKRMDKAGQYTDKGLR-KCEDGMRDIP -MRYSCORRRLITQ -GESLKAAMDCCNYITKLRQHRRDHV-LGLAR
 -SVRLIKHGTKMAEYSDKNLR-KCEDGIRKNL -MGYSCERMTYVLD -AKSDEAFLSCCLYIKGHRDRELEQ--YELAR
 SSVLLDSSKASAAQFDQGLR-KCEDGMHENP -MGYCEKRKMYIQE -GDAKRAAFLECCHYIKGHRDRESE--LFLAR
 SSVALLIKSGKASFYK-DKAK-KCCLDGAQENL -LGHICDRRARIYILD -GKEQVDAFVDCCKYYEKREAEKISKDD-DLTLGR
 -ATTVMNVTTLVYKYNELQR-ECCSEGMKETT -LGYICEVRSYIELD -GASQVDAFVDCCKEMERHREMKQDQ--LTLGR
 -AVTLDVITSMASKYH-GLAK-ECCVDGMRDNT -LGYICDRRAQYISD -GDVQVAFVDCCKEMASKIESKQDA--LILSR
 -BESTLQITSTLVGKYS-GELK-ECCIDGMRENK -LGYICERRMYIVD -GQKAKVELHCCNEIKTRKMKTEEEE--MILAR
 -NVMFQKRAINEKLGQYASPTAK-KCQDGVTRLP -MRSCEORARVQQ --PDGREPFLSCQFAE SFRKKS RDKGQ--AGLQR
 RNVMFQKRAINEKLGQYASPTAK-KCQDGVTRLP -MRSCEORARVQQ --PDGREPFLSCQFAE SFRKKS RDKGQ--AGLQR
 -NVMFQKAVSEKLGQYSSPDAK-KCQDGMTKLP -MKLICEORARVQQ --QAGREPFLSCCKFAEDLRNQRSQ--AHLAR
 RSLBELKLEEKAGPARNHTMRCRCDGATAIP -IRAIQOORGQVTTI -AGGQVDAFVDCCEVAQHRLRQGRG--GLAR
 RSDIDQEMNRLKSGYEDTELO-LCQAQAFSLIP -MKRICEERARVRL -VGGSEAGAAAEKCCCTETEILRRKILEEGQ-SGFGR
 RSDIDQEMLSLKYNITDKSLO-ECCAKGFSLIP -MRRICEERAQRIISL -MEGQSPQVEVELHCCRKGEHLRQKMKEDAR-KGTLGR
 RSLDIDQEMVSKSSYSDAKLO-ECCSHGLSLIA -MLRICEORARVRL -ANKDRYVKAFLDCCIEGEKLEKRRKDDAQ-SGHGR
 RALDIDQALTOQKAYSITTELO-KCQHGMLPPEKSRVYTKRARVDP -PTCRKAFLDCCFYAEHLRQLTLEKRTQGFGR
 RALMIDQOYAGKLNRYTDRLR-KCYTDGLTKIL -MPSHEERISRKE --LDGRVFOCKCDYGVLEKQSLKV--DSLAR
 KRELIDLEIAIEKASTYP-AELR-KCQRDAIESP -LRLSBERUKHIHD -EGEQVTEIECCKHVEEELIAMEEED-EDLGR
 -RQJSMLOIRREAEKYT-QEFR-KCQVDGLKMSPP -TGQGCBERLKRVTG --PKKQVDAFVDCCKKAAEYRKSSELGAK--TVLRR
 ---TQCKIEEIAAKYKHSVVK-KCQYDGACVNN -DEICEORARISL -GPRKIKAFTECCVVASQLRANISHKD--MQJGR
 -RMQCKKIEEIAAKYAMLK-KCQYDGAYRND -DEICEORARIKI -GPKQVKAFLDCCYIANQVRAEESHKN--IQJGR
 DLQJHQKVEEIAAKYKHRVPK-KCQYDGARENK --YEICEORVARVTI ---GPHGIRAFKECCTIADHIREKNE SHKG--MLLGR
 --HLRQKIEEIAAKYKHSVVK-KCQYDGARVNF --YEICEERVARVTI ---GLPISIRAFNECCTIANKIRKQSPHPK--VQJGR
 ---SFDDKRIEALNSKNIWVR-KCCLDGMKGYPP -TEFICEVWRAGRIKD -RKFLPRQIEAEKRCCRLVEEEDYTGKT--LELAR
 RKRDIDQNSLEAKVMEFN-ETLO-PCQMDGQWDDP -LGRSCLQRKLNST --SQDESYFAFLTCCNHARSIRLRIGRGG--RGR
 -IRKKRIMEEIVKQYE-KRDK-QCCILGMKHDPP -DQRSCEERHAIFEKYDFDGKETGMARFLG -CCNEKHYLLNIEKE--GRGR
 -SRKKPQLOVEQELSIE-AKLIH-KCEDGKKKKSFS-ECDLICEMORDRVIYTFDDDAIPGCSERYAEIALARLMSGTRRQR--VQGR

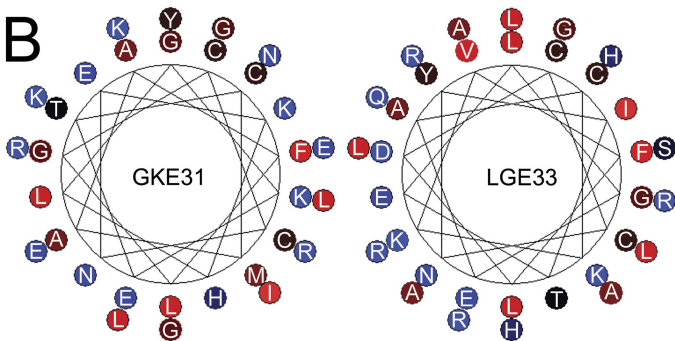
- C3aHomo
- C3aGumiea
- C3aSus
- C3aMus
- C3aRattus
- C3aGallus
- C3aNaJna
- C3aXenopus
- C3aParalichthys
- C3aOncorhynchus
- C3aCtenopharyngodon
- C4aHomo
- C4aPantroglydotes
- C4aMus
- C4aGallus
- C4aOryzias
- C4aTakiFugu
- C4aOncorhynchus
- C4aXenopus
- C4aTriakis
- C3aEptatretus
- C3aLethenteron
- C5aHomo
- C5aSus
- C5aRattus
- C5aMus
- C5aNotophthalmus
- C3aBranchiostoma
- C3aCarcinoscorpius
- C3aCiona

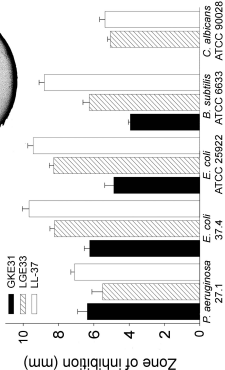
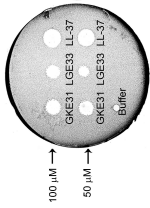
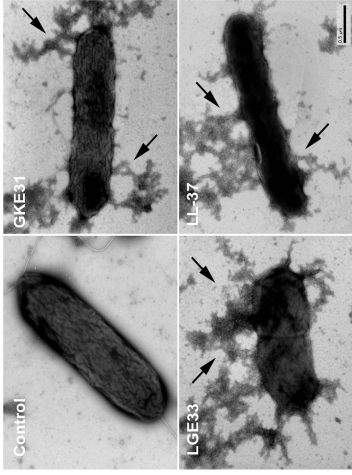
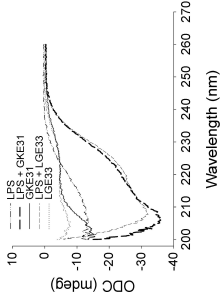
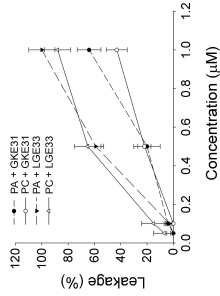
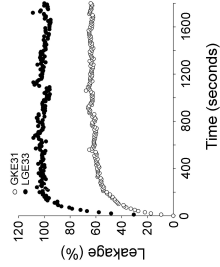
AC3a *C. rotundicauda*

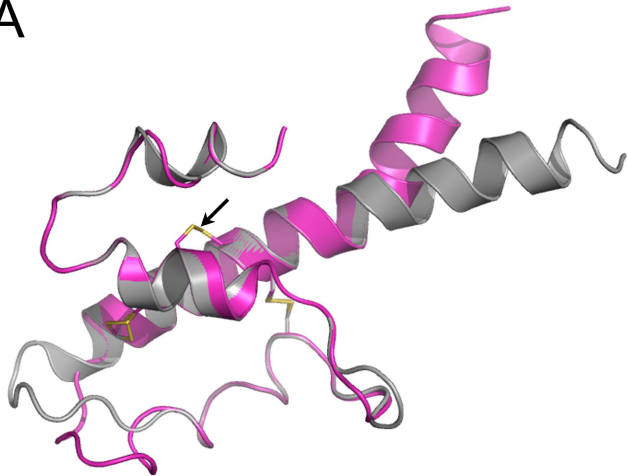
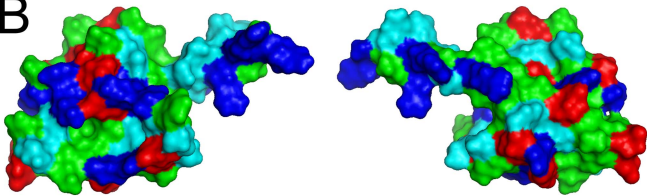
C3a Homo

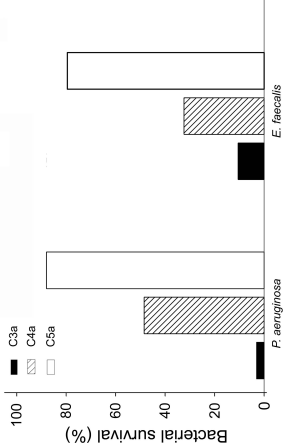
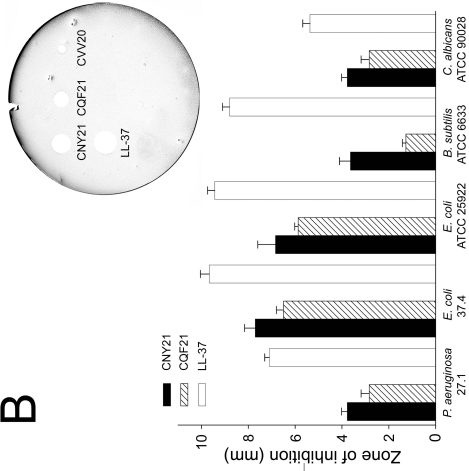
C4a Homo

C5a Homo

B

A**B****C****D****E**

A**B**

A**B****C**